THE JOURNAL OF BIOLOGICAL CHEMISTRY
Vol. 275, No. 39, Issue of September 29, pp. 30058–30063, 2000
Printed in U.S.A.

Eukaryotically Encoded and Chloroplast-located Rubredoxin Is Associated with Photosystem II*

Received for publication, May 29, 2000, and in revised form, June 28, 2000
Published, JBC Papers in Press, June 30, 2000, DOI 10.1074/jbc.M004629200

Jürgen Wastl‡, Evert C. Duin§, Lucia Iuzzolino‡, Wolfgang Dörner‡, Thomas Link¶, Silke Hoffmann‖, Heinrich Sticht‖, Holger Dau, Klaus Lingelbach‡, and Uwe-G. Maier‡ ‡‡**

*From the ‡Fachbereich Biologie, Philipps-Universität Marburg, Karl-von-Frisch-Strasse, D-35032 Marburg, §Max Planck Institut für Terrestrische Mikrobiologie, Karl-von-Frisch-Strasse, D-35043 Marburg, ¶Institut für Biophysik, Universität Frankfurt, Theodor-Stern-Kai 7, D-60590 Frankfurt/Main, ‖Lehrstuhl für Biopolymere, Universität Bayreuth, Universitätsstrasse 30, D-95440 Bayreuth, and **Institut für Experimentalphysik, Fachbereich Physik der Freien Universität Berlin, Arnimallee 14, D-14195 Berlin, Germany*

We analyzed a eukaryotically encoded rubredoxin from the cryptomonad *Guillardia theta* and identified additional domains at the N- and C-termini in comparison to known prokaryotic paralogous molecules. The cryptophytic N-terminal extension was shown to be a transit peptide for intracellular targeting of the protein to the plastid, whereas a C-terminal domain represents a membrane anchor. Rubredoxin was identified in all tested phototrophic eukaryotes. Presumably facilitated by its C-terminal extension, nucleomorph-encoded rubredoxin (nmRub) is associated with the thylakoid membrane. Association with photosystem II (PSII) was demonstrated by co-localization of nmRub and PSII membrane particles and PSII core complexes and confirmed by comparative electron paramagnetic resonance measurements. The midpoint potential of nmRub was determined as +125 mV, which is the highest redox potential of all known rubredoxins. Therefore, nmRub provides a striking example of the ability of the protein environment to tune the redox potentials of metal sites, allowing for evolutionary adaption in specific electron transport systems, as for example that coupled to the PSII pathway.

Rubredoxin is a non-heme iron protein, in which one iron is tetrahedrally coordinated by four cysteines (1). In anaerobic as well as aerobic bacteria, rubredoxin acts as a cofactor in several biochemical pathways. For example, in *Azotobacter vinelandii* rubredoxin participates in hydrogen oxidation (2), and, as recently described, it acts as an electron acceptor for pyruvate ferredoxin oxidoreductase in *Chlorobium tepidum* (3). As shown by the sequencing of the *Synechocystis* sp. PCC6803 genome (4), a rubredoxin gene is encoded in the cyanobacterial genome as well. In contrast to other bacterial rubredoxins, the *Synechocystis* gene encodes a C-terminal extension, which was predicted to be a membrane anchor.

Cryptomonads are small unicellular biflagellated algae. In addition to the nucleus, the plastid, and the mitochondrion, a fourth DNA-containing organelle, the nucleomorph, was identified (5). The genome of the nucleomorph ranges from 520 to 660 kilobases and is arranged in three tiny chromosomes.[1] Phylogenetic studies have demonstrated that the nucleomorph represents the vestigial nucleus of a former free living red algae, which was engulfed and reduced to a secondary endocytobiont.[1]

In the course of an international effort to sequence the nucleomorph genome of the cryptomonad *Guillardia theta* (7), a nucleomorph-located and therefore eukaryotically encoded rubredoxin gene was identified (8, 9). Here, we present data concerning the characterization of the encoded protein by means of immunological and biochemical methods and show the intracellular localization of rubredoxin as well as its redox properties. We present evidence that *G. theta* rubredoxin shows similar EPR[2] spectra to those of the bacterial paralogous proteins, indicating a redox active iron atom. Measurements of its redox potential gave a value of +125 mV, which is the highest potential of all rubredoxins investigated so far. Furthermore we demonstrate that rubredoxin is plastid-located and anchored into the thylakoid membranes. Additionally, we present evidence that rubredoxin is associated with photosystem II (PSII) by co-localization of rubredoxin in BBYs and OG and DM cores.

MATERIALS AND METHODS

Recombinant Protein and Antibodies—Overexpression and purification of a 70-amino acid recombinant rubredoxin was done as described previously (8). To raise a polyclonal antiserum against recombinant rubredoxin, 1 mg of the purified protein was used to immunize a rabbit.

Preparation of Crude Extracts, SDS-PAGE, Blotting, and Immunodetection—Protein extracts were prepared by boiling the samples in extraction buffer containing 3% (w/v) SDS, 0.2% (w/v) Triton X-100, and 125 mM Tris-HCl (pH 6.8). Denatured proteins were separated by SDS-PAGE (10). Subsequently, proteins were transferred to nitrocellulose membranes (Schleicher & Schuell, 0.2 μm) by semidry blotting. The primary antibody was detected by a secondary anti-rabbit antibody conjugated with horseradish peroxidase. Immunodetection was undertaken with the ECL system according to the manufacturer's protocol (Amersham Pharmacia Biotech).

Preparation of Plastids, Thylakoids, and Photosystem II Complexes—Plastids from *Pisum sativum* were purified by means of density gradient centrifugation according to Wastl and Maier (11). Intact thylakoid membranes from *P. sativum* were isolated by purification of chloroplasts (12) and subsequent "smooth" disruption of the chloroplasts (0.1% Triton X-100) for 5 min on ice.

* This work was supported by grants from the Deutsche Forschungsgemeinschaft. The costs of publication of this article were defrayed in part by the payment of page charges. This article must therefore be hereby marked "*advertisement*" in accordance with 18 U.S.C. Section 1734 solely to indicate this fact.

‡‡ To whom correspondence should be addressed. E-mail: maier@mailer.uni-marburg.de.

[1] Maier, U.-G., Douglas, S. E., and Cavalier-Smith, T. (2000) *Protist*, in press.

[2] The abbreviations used are: EPR, electron paramagnetic resonance; PSII, photosystem II; BBY, PSII-enriched membrane fragments (method developed by Berthold, Babcock and Yocum); OG, *n*-octyl-β-D-glycoside; DM, *n*-dodecyl-β-D-maltoside; SDS-PAGE, SDS-polyacrylamide gel electrophoresis; GlyB, glycine betaine; MES, 4-morpholineethanesulfonic acid; nmRub, nucleomorph-encoded rubredoxin.

PSII-enriched membrane fragments were prepared as described previously (13). The protocol for the preparation of *n*-octyl-β-D-glycoside-solubilized PSII core particles ("OG cores") and PSII core dimers described by Hankamer *et al.* (14) was modified in that the osmoprotective agent glycine betaine (GlyB) was used throughout the preparation. The modified procedures for OG cores are described in Dörner *et al.* (15). For PSII core dimers 1 M GlyB was present in the resuspension and solubilization buffer (1 M GlyB, 25 mM MES, 10 mM NaCl, 5 mM $CaCl_2$, pH 6.0), whereas the sucrose gradient solution contained 2 M GlyB (2 M GlyB, 25 mM MES, 10 mM NaCl, 5 mM $CaCl_2$, 0.03% (w/v) *n*-dodecyl-β-D-maltoside, pH 6.0, and 0–10% sucrose) (16). PSII dimer samples were concentrated by means of a Microsep membrane concentrator (100-kDa cutoff, Pall Filtron).

Immunogold Microscopy—Cells from *G. theta* and *Synechocystis* sp. PCC6803 as well as thylakoid preparations were embedded in Lowicryl K4M (Chemische Werke Lowi) according to the instructions of the manufacturer. After ultrathin cutting, the sections were incubated with a polyclonal rabbit antiserum raised against recombinant *G. theta* rubredoxin. Gold-labeled goat anti-rabbit IgG was used for detection of the primary antibodies as described in Fraunholz *et al.* (17).

Import Experiments—Transport-competent plastids were isolated by means of differential density gradient centrifugation, as described previously (11). *In vitro* transcription and translation of the constructs were performed using the coupled reticulocyte transcription/translation system (TNT system, Promega). Translation of the template was performed in the presence of [^{35}S]methionine (1000 Ci/mmol, Amersham Pharmacia Biotech) according to the manufacturer's protocol.

Posttranslational import of labeled precursor proteins into *P. sativum* plastids took place in 100-μl assays containing plastids (equivalent to 15 μg of chlorophyll) in import buffer containing 2 mM ATP, 20 mM potassium gluconate, 10 mM methionine, 10 mM $NaHCO_3$, and 2% bovine serum albumin.

After addition of labeled *in vitro* translation product, the import mixture was incubated 30 min at 25 °C with pea plastids. The reaction was terminated by centrifugation of the chloroplasts for 1 min at 1000 × *g*. After washing in import buffer, chloroplasts were resuspended in 100 μl of import buffer and subjected to thermolysin treatment (0.1% (w/v) thermolysin, Roche Molecular Biochemicals) with a 1 mM $CaCl_2$ final concentration for 10 min on ice to digest external protein of the import mixture. The digestion was stopped by adding EDTA to a final concentration of 5 mM; this was followed by centrifugation through a 40% percoll cushion (4500 × *g*, 5 min) to recover intact plastids. After washing and centrifuging the plastids, harvested chloroplasts were resuspended immediately in sample buffer for analysis by SDS-PAGE and subsequent autoradiography.

EPR Spectroscopy—EPR spectra at X-band (9 GHz) were obtained with a Bruker EMX-6/1 EPR spectrometer composed of the EMX 1/3 console, ER 041 X6 bridge with built-in ER-0410–1161 microwave frequency counter, ER-070 magnet, and ER-4/02 st standard universal TE102 rectangular cavity. All spectra were recorded with a field modulation frequency of 100 kHz. Cooling of the sample was performed with an Oxford Instruments ESR 900 cryostat with a ITC4 temperature controller.

Electrochemistry—Cyclic voltammetry was performed at a nitric acid-modified glassy carbon electrode using the setup described by Hagen (18). To remove O_2, the assembled cell was flushed with argon. A 12-μl sample of approximately 100 μM protein in 50 mM potassium phosphate buffer, pH 7, was inserted through a septum and placed so that it formed a drop between the working, reference, and counter electrodes. Cyclic voltammograms of rubredoxin were recorded at scan rates of 10–100 mV/s using a computer-controlled Autolab PGSTAT-10 potentiostat. Midpoint potentials were determined from the anodic and cathodic peak potentials.

RESULTS

As recently published, we have isolated a gene encoding rubredoxin from the cryptomonad *G. theta*. It is localized on chromosome II of the remnant nucleus of the secondary endosymbiont, the nucleomorph (8, 9). In the conserved positions rubredoxin (nmRub) has high identity to prokaryotic paralogous molecules (Fig. 1), which were identified in several anaerobic and aerobic eubacteria (8). The cyanobacterium *Synechocystis* harbors a rubredoxin gene that encodes a hypothetical protein with an additional C-terminal extension (Fig. 1). This extension was predicted to be a membrane anchor. A similar C-terminal membrane anchor was also identified in the cryptomonad rubredoxin protein as well as in an *Arabidopsis* expressed sequence tag clone (Swiss-Prot accession number AAD25628). Unique to the eukaryotically encoded rubredoxins in *G. theta* and *Arabidopsis* is an N-terminal extension (Fig. 1), which resembled a transit peptide. Nevertheless, data base searches failed to predict the N-terminal extension of the *G. theta* rubredoxin as a transit peptide.

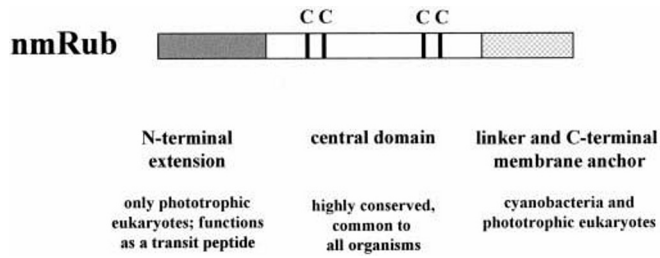

FIG. 1. **Domains of the rubredoxins.** Shown are the N-terminal extension (*dark gray*), which is essential for protein translocation across the plastid envelope, the central, iron binding domain with four highly conserved cysteines (*C*), and the C-terminal-located hydrophobic domain (*light gray*), which is responsible for anchoring rubredoxin to membranes in aerobic photosynthetic organisms.

In Vitro Import Assays of G. theta Rubredoxin—Because the N-terminal extension of the nmRub is not predicted to be a transit peptide, we undertook *in vitro* import assays into isolated plastids. As shown in Fig. 2, rubredoxin precursors can be imported into chloroplasts from *P. sativum*. This is demonstrated by the finding that the *in vitro* translation product, when incubated with chloroplasts, was processed to the mature protein, which was thermolysin-resistant as long as the chloroplasts were intact but was digested if thermolysin and Triton X-100 were added to the reaction mixture. Therefore, the N-terminal extension of the nucleomorph-encoded rubredoxin represents a transit peptide, and nmRub has a plastid destination at least in *in vitro* experiments.

Detection and Localization of Rubredoxin by Use of an Antiserum—In addition to the import studies presented above, further experiments to localize rubredoxin were done. We used a recombinant and purified cryptomonad rubredoxin protein (8) for the generation of polyclonal antibodies.

In Western blot experiments with these antibodies a single band of approximately 11 kDa could be identified in *G. theta* protein extract, which corresponded to the size of mature rubredoxin (Fig. 3). By the use of this antibody, a band of identical molecular mass was also detectable in *Synechocystis* and *Arabidopsis thaliana*. Interestingly, in protein extracts from *Chilomonas paramecium*, a heterotrophic cryptomonad alga with a photosynthetic inactive leucoplast, the polyclonal antiserum did not detect any protein (data not shown).

To localize the protein within the algal cell, electron microscopical immunolocalization experiments were undertaken. Cells were embedded in ultrathinly cut Lowicryl, and the localization of rubredoxin was visualized by means of the immunogold technique. A specific label at the internal membrane system, the thylakoids, was detected in *G. theta* as well as in *Synechocystis* (Fig. 4, *A* and *B*).

A similar result was obtained in immunogold experiments with isolated pea thylakoids. As shown in Fig. 4*C*, both stroma and grana thylakoids were labeled. Counting the labels of both types of thylakoids separately, 80% of the gold particles were associated with the grana thylakoids, and 20% had a stroma thylakoid localization. This observed grana to stroma ratio of nmRub corresponded to the distribution of PS II complexes in the thylakoid membrane system of chloroplasts (19).

Furthermore, whole cells, isolated plastids, and thylakoids were used to specify the orientation of rubredoxin within the

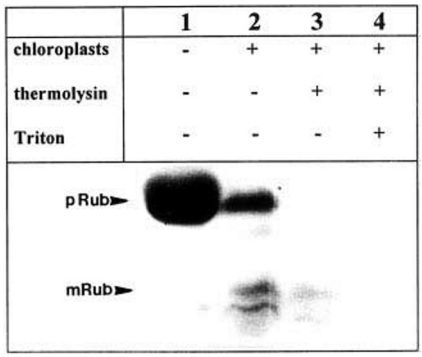

FIG. 2. **Import of rubredoxin precursor into pea plastids.** An autoradiography of 17% SDS-PAGE is shown. *Lane 1* shows the full-length translation product of nucleomorph-encoded rubredoxin (indicated by *pRub*). *Lane 2* corresponds to the protein pattern after the import reaction of [^{35}S]methionine-labeled precursor protein pRub. The processed protein is indicated by *mRub*. *Lane 3* represents a reaction in which the pea chloroplasts were treated with thermolysin after the import reaction. The protease resistant band is shown. *Lane 4* shows the experiment as in 3 with additional Triton X-100 prior to protease treatment.

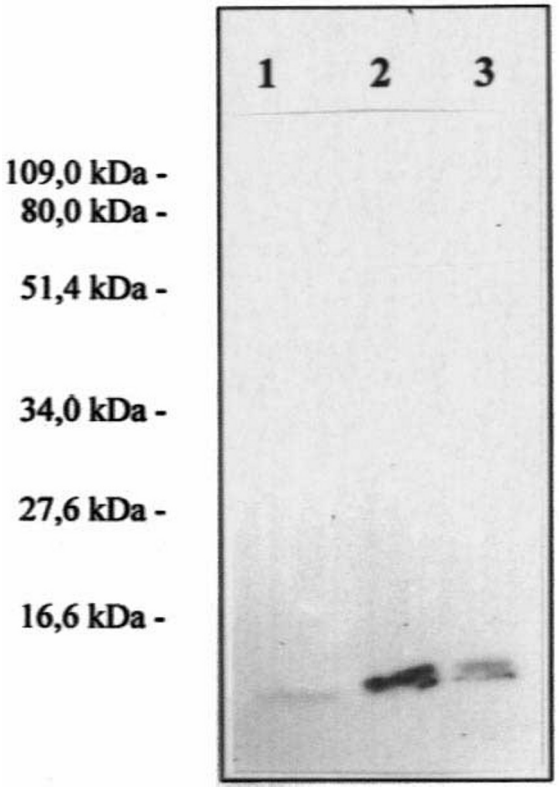

FIG. 3. **Immunodetection of protein extracts with an anti-rubredoxin antiserum.** Protein crude extracts (corresponding to 50 μg) of *A. thaliana* (*lane 1*), the cyanobacterium *Synechocystis* sp. PCC6803 (*lane 2*), and the cryptomonad *G. theta* (*lane 3*) were separated by SDS-PAGE (15%), blotted, and incubated with anti-rubredoxin antiserum. Immunodetection was done by ECL. An band of approximately 11 kDa is shown, corresponding to the mass of mature rubredoxin.

thylakoid system. For these experiments the extracts were incubated with and without thermolysin and Triton X-100, and the presence of rubredoxin was analyzed by Western blotting and immunodetection. Our data suggest that rubredoxin is an integral thylakoid protein whose soluble domain is exposed to the stroma (data not shown).

Localization of Rubredoxin in BBY, OG, and DM Cores—The localization of rubredoxin in thylakoids, as well as the fact that rubredoxin has a similar distribution to that of photosystem II complexes, suggested a co-localization of rubredoxin with PS II. To test if rubredoxin is attached to the photosynthesis machinery or is a part of it, we isolated PS II-enriched complexes from spinach thylakoids. One fraction consisted of the so-called BBYs, which are enriched in photosystem II but nearly free of photosystem I components (20). Depletion of light-harvesting complex II from the BBYs using detergents led to OG cores (21) and light-harvesting complex II-free DM cores. The latter resembled the purified PSII core complex (14). These particles still showed O_2-evolving activity (data not shown). In Western blots the anti-rubredoxin antibody specifically detected a protein with identical molecular mass as nmRub in BBYs and OG and DM cores, indicating that rubredoxin is associated with the photosystem II machinery (Fig. 5).

Comparative EPR Studies—In previous studies we could show that nmRub is an iron-containing protein (8). However, neither by UV-visible spectroscopy nor by 1D NMR analysis was it possible to determine the coordination state of the iron cofactor of nmRub. Therefore we determined the state of the iron cofactor in the oxidized recombinant cryptomonad rubredoxin by EPR. As shown in Fig. 6, the cryptomonad protein had peaks at $g = 9.6$ and $g = 4.3$, identical to those of *Clostridium pasteurianum* rubredoxin. Thus, the four cysteines of nmRub probably coordinate an iron atom tetrahedrally and therefore in the same manner as prokaryotic rubredoxins (*e.g.* Ref. 22).

The presented immunological data (see "Detection and Localization of Rubredoxin by Use of an Antiserum") supposed a co-localization of rubredoxin with PSII. Previous EPR studies on enriched PS II complexes revealed an additional characteristic iron peak at $g = 4.3$, which has been explained as iron contamination (23). It is possible, however, that this signal, or part of it, is due to the rubredoxin. The shape of the signal having a g value of 4.3 is predominantly rhombic. This might be because of the association of the rubredoxin to the membranes. Saturation studies (data not shown) of the signals with g values of 4.3 in the nmRub preparation and the enriched PS II preparation show very similar behavior, and for example at 4.6 K the signals start to saturate at around 2 milliwatts. In comparison the signals with a g value of 4.3 of adventitiously bound iron in bovine serum albumin or lysozyme preparations start to saturate at around 0.2 milliwatts and 20 microwatts, respectively. Adventitiously bound iron is expected to be coordinated by less than four ligands, which are probably oxygen or nitrogen, and will behave differently in saturation and temperature studies than iron coordinated by four cysteine ligands. More evidence is required, however, and EPR-monitored redox titration should be able to prove whether this signal with a g value of 4.3 in the enriched PSII preparation is due to rubredoxin.

Redox Potential—To characterize the electrophysiological properties of the cryptomonad rubredoxin, we determined its redox potential under the same conditions as in Eidsness *et al.* (22). Purified recombinant rubredoxin (8) was used to measure the redox potential. The midpoint reduction potential of recombinant *G. theta* rubredoxin was determined as +125 mV. In comparison to all other known rubredoxins, which yield redox potentials of approximately −50 mV to +50 mV, the cryptomonad rubredoxin revealed the highest redox potential known so far. Interestingly, the redox potential of the cryptomonad rubredoxin is similar to those of the cytochrome b_6/f complex and plastoquinone.

DISCUSSION

Rubredoxin is a small non-heme iron protein known from anaerobic and aerobic bacteria. The identification of the first eukaryotically encoded rubredoxin gene in the nucleomorph of

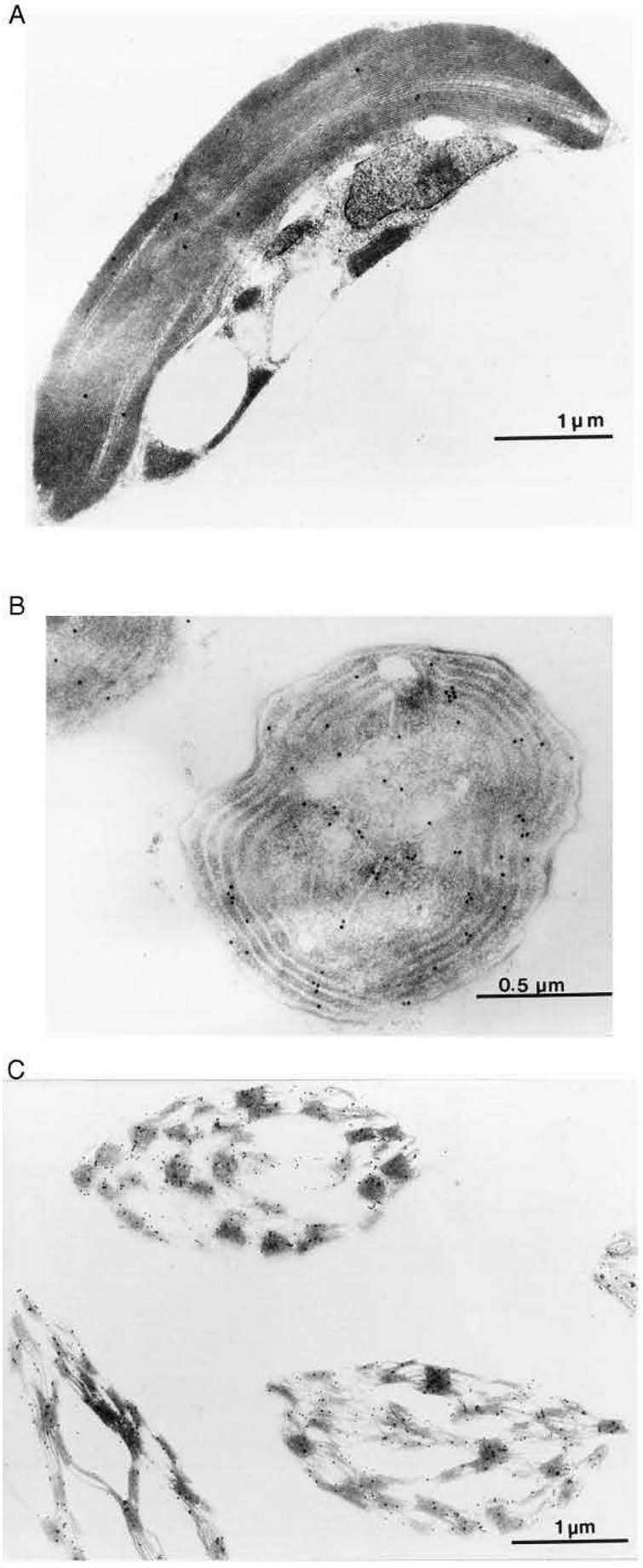

FIG. 4. **Electron microscopical *in situ* localization of rubredoxin.** Ultrathin sections of the cryptomonad *G. theta* (*A*), *Synechocystis* sp. PCC6803 (*B*), and thylakoids from *P. sativum* (*C*) were incubated with a polyclonal antiserum raised against recombinant *G. theta* rubredoxin. 15-nm gold-conjugated goat anti-rabbit IgG secondary antibodies were used to visualize the localization of rubredoxin.

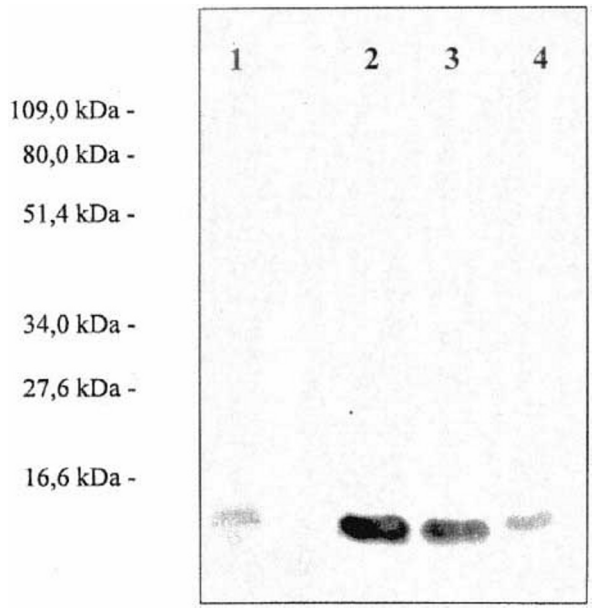

FIG. 5. **Immunodetection of rubredoxin in photosystem II-enriched complexes.** Photosystem II complexes were enriched, leading to BBY particles, OG core complexes, and dimers of PSII after an additional ultracentrifugation. The probes (corresponding to 3 μg of chlorophyll *a*) were separated by SDS-PAGE (15%), blotted on nitrocellulose membranes, and incubated with anti-rubredoxin antiserum. Immunodetection was done by means of ECL. In *G. theta* (*lane 1*) as well as in the PSII preparations (the BBY particles (*lane 2*), the OG core complexes (*lane 3*), and the PSII dimers (*lane 4*)) a specific label of a protein corresponding to mature rubredoxin was detected.

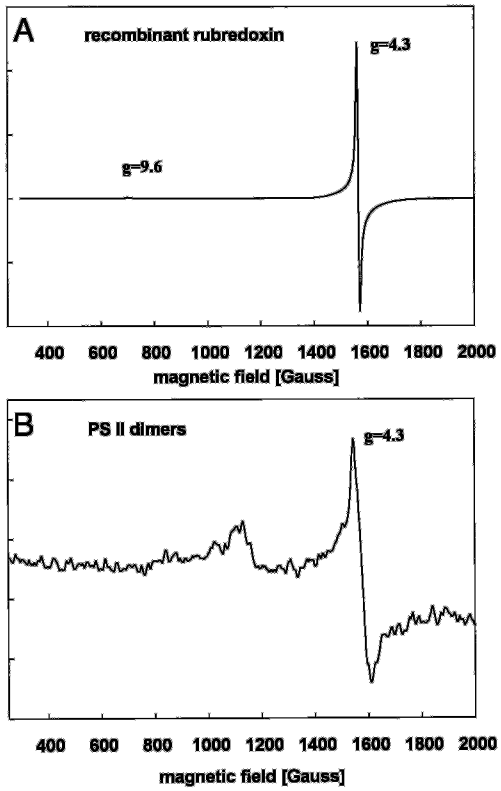

FIG. 6. **Comparative EPR measurements of recombinant *G. theta* rubredoxin and *S. oleracea* photosystem II complexes.** *A* shows the EPR measurement of recombinant rubredoxin in its oxidized form at 4.5 K. The typical bands of a rhombic, non-heme iron are visible. Under identical conditions as in *A*, enriched photosystem II complexes (PSII core dimers) from *S. oleracea* revealed a similar signal at g = 4.3 (*B*).

cryptomonads (9) raised the question whether this polypeptide is similar in function to the bacterial ones.

Analysis of the primary structure revealed an N- and C-terminal extensions of the cryptomonad protein in comparison to prokaryotically encoded rubredoxins. The N-terminal extension was shown to be a transit peptide in the homologous system (11) and a heterologous system (this study), and this extension directs the protein to *G. theta* plastids.

According to our results the C-terminal domain acts as a membrane anchor. This membrane anchor is a characteristic feature of all other known rubredoxin genes in all known photosynthetic organisms, supporting a conserved linkage of rubredoxin to a plastid membrane. Because only a limited set of data exists concerning the existence of rubredoxin in other organisms, we used a polyclonal antibody raised against the recombinant *G. theta* rubredoxin to determine whether rubredoxin is common in higher plants. As shown in Fig. 3, a cross-reacting band with a molecular mass identical to that of mature rubredoxin was present in cyanobacteria, cryptomonads, and higher plants, whereas it was missing in a non-photosynthetic cryptomonad. Thus, this is the first evidence that rubredoxin is common to photosynthetically active eukaryotes and cyanobacteria.

By the use of an anti-rubredoxin antibody and an immunogold-labeled secondary antibody as well as Western experiments, we demonstrated that rubredoxin is integrated into the thylakoid membranes and exposed to the stroma. In *Synechocystis*, rubredoxin is located in an operon together with components of PSII. This fact, together with our electron microscopical immunolocalizations, which show that rubredoxin is mainly located in grana thylakoids, suggested that rubredoxin is attached to PSII. To test this we prepared thylakoid membranes from *Spinacia oleracea* and from these enriched PSII preparations. Whereas the BBYs contain PSII together with the light-harvesting complexes, plastoquinone, and partial cytochrome b_6/f complexes, the DM core complexes are membrane-free and resemble pure PSII complexes without the light-harvesting complexes, cytochrome b_6/f complex, or plastoquinone. In these preparations the anti-nmRub antibody detected a protein with the molecular mass of rubredoxin, strongly indicating that the iron protein is connected to PSII.

Interestingly, in PSII-enriched membrane particles an EPR signal characterized by a g value around 4 is always observed. Previously, this EPR signal was thought to result from adventitious iron contamination (23). However, we detected a narrow EPR signal exactly at the rubredoxin g value of 4.3 in repeatedly washed PSII membrane particles (not shown) as well as in the even more purified PSII core complexes (Fig. 6). Thus the observed EPR signal with a g value of 4.3 is not an iron artifact but is probably related to rubredoxin, which is closely associated with PSII.

These facts raised a question concerning the function of rubredoxin in PSII. Ycf48, formerly known as Hcf136, is essential for the assembly of the PSII components in the thylakoid membrane (24). In addition, PsbE is essential in the process of PSII assembly, as shown by Morais *et al.* (25) for a *psb*E null mutant from *Chlamydomonas reinhardtii*. Both proteins are involved in the assembly process but could not be detected in mature PSII complexes. Our immunological data showed that rubredoxin is associated with mature PSII in stroma and grana thylakoids. Thus rubredoxin seems not to be involved, at least in the early steps of PSII assembly.

The characterization of the central iron ligation domain is essential for the understanding of the function of rubredoxins in photosynthetic organisms. An alignment of different rubredoxins suggested the chelation of an iron molecule by four highly conserved cysteines (8). This iron is responsible for the

ability of rubredoxins to take part in redox reactions, as it was shown *e.g.* for *A. vinelandii* rubredoxin (2).

EPR spectroscopy of recombinant nmRub gave the same g values as those observed for other rubredoxins, indicating that nmRub contains high spin Fe^{3+} in almost tetrahedral coordination. Because rubredoxin acts as an electron carrier, knowledge of its redox potential is important. We showed that its redox potential was +125 mV and therefore the highest redox potential of all rubredoxins known so far. This redox value, which is similar to those of the cytochrome b_6/f complex and plastoquinone, implies that rubredoxin is able to branch electrons from, or replace components of, PSII.

According to Eidsness *et al.* (22) and Xiao *et al.* (26), all rubredoxins can be divided into two groups with respect to their redox potentials. The reason for this is a crucial amino acid at a conserved position (amino acid residue 44, referring to *C. pasteurianum* rubredoxin). Site-directed mutagenesis showed that changes from valine to the more polar alanine (and *vice versa*) correlate with the change of midpoint redox potential (22). Exclusively, the *G. theta* rubredoxin sequence has a serine at this position. Further structural characterization of the recombinant *G. theta* rubredoxin by NMR showed the closeness of the neighborhood of the serine to the four iron-ligating cysteines.[3] Therefore it is likely that the presence of serine (which is even more polar than alanine) in this position is responsible for the high midpoint potential of nmRub. Similar effects have been observed in the case of 2[4Fe-4S] ferredoxins (6).

Our data confirm that rubredoxin found in organisms with oxygenic photosynthesis is a plastid-located protein integrated into the thylakoid membranes and exposed to the stroma. Immunogold localizations gave hints that rubredoxin is associated with photosystem II, which was confirmed by co-localizations of rubredoxin with purified PSII core complexes. The typical arrangement of the central iron atom and the determined redox potential of +125 mV led to the conclusion that rubredoxin could act as an electron transfer molecule branching electrons from PSII to plastid membrane-located pathways (*e.g.* xantophyll cycle and fatty acid biosynthesis) or could replace the cytochrome b_6/f complex or plastoquinone of the photosynthesis machinery under some circumstances.

Acknowledgments—We thank Marianne Johannsen and Lothar Kremp for technical assistance.

[3] Schweimer, K., Hoffmann, S., Wastl, J., Maier, U.-G., Rösch, P., and Sticht, H. (2000) *Protein Sci.*, in press.

REFERENCES

1. Meyer, J., Gaillard, J., and Lutz, M. (1995) *Biochem. Biophys. Res. Commun.* **212,** 827–833
2. Chen, J. C., and Mortenson, L. E. (1992) *Biochim. Biophys. Acta* **1131,** 122–124
3. Yoon, K.-S., Hille, R., Hemann, C., and Tabita, F. R. (1999) *J. Biol. Chem.* **274,** 29772–29778
4. Kaneko, T., Sato, S., Kotani, H., Tanaka, A., Asamizu, E., Nakamura, Y., Miyajima, N., Hirosawa, M., Sugiura, M., Sasamoto, S., Kimura, T., Hosouchi, T., Matsuno, A., Muraki, A., Nakazaki, N., Naruo, K., Okumura, S., Shimpo, S., Takeuchi, C., Wada, T., Watanabe, A., Yamada, M., Yasuda, M., and Tabata, S. (1996) *DNA Res.* **3,** 109–136
5. Gibbs, S. P. (1981) *Ann. N. Y. Acad. Sci.* **361,** 193–208
6. Kyritsis, P., Hatzfeld, O. M., Link, T. A., and Moulis, J. M. (1998) *J. Biol. Chem.* **273,** 15404–15411
7. Gilson, P. R., Maier, U.-G., and McFadden, G. I. (1997) *Cur. Opin. Genet. Dev.* **7,** 800–806
8. Wastl, J., Sticht, H., Maier, U.-G., Rösch, P., and Hoffmann, S. (2000) *FEBS Lett.* **471,** 191–196
9. Zauner, S., Fraunholz, M., Wastl, J., Penny, S., Beaton, M., Cavalier-Smith, T., Maier, U.-G., and Douglas, S. (2000) *Proc. Natl. Acad. Sci. U. S. A.* **97,** 200–205
10. Laemmli, U. K. (1970) *Nature* **227,** 680–685
11. Wastl, J., and Maier, U.-G. (2000) *J. Biol. Chem.* **275,** 23194–23198
12. Schindler, C., Hracky, R., and Soll, J. (1987) *Z. Naturforsch.* **42,** 103–108
13. Iuzzolino, L., Dittmer, J., Dörner, W., Meyer-Klaucke, W., and Dau, H. (1998) *Biochemistry* **37,** 17112–17119
14. Hankamer, B., Nield, J., Zheleva, D., Boekema, E. J., Jansson, S., and Barber, J. (1997) *Eur. J. Biochem.* **243,** 422–429
15. Dörner, W., Dittmer, J., Iuzzolino, L., Meyer-Klaucke, W., and Dau, H. (1998) in *Photosynthesis: Mechanisms and Effects* (Garab, G., ed) Vol. II, pp. 1343–1346, Kluwer Academic Publishers, Dordrecht, The Netherlands
16. Catucci, L., Dörner, W., Nield, J., Hankamer, B., Vass, I., and Barber, J. (1998) in Photosynthesis: Mechanisms and Effects (Garab, G. ed.), Vol. II, pp. 973–976, Kluwer Academic Publishers, Dordrecht, The Netherlands
17. Fraunholz, M. J., Mörschel, E., and Maier, U.-G. (1998) *Mol. Gen. Genet.* **260,** 207–211
18. Hagen, W. R. (1989) *Eur. J. Biochem.* **182,** 523–530
19. Staehelin, L. A., and DeWit, M. (1984) *J. Cell. Biochem.* **24,** 261–269
20. Berthold, D. A., Babcock, G. T., and Yocum, C. F. (1981) *FEBS Lett.* **134,** 231–234
21. Ghanotakis, D. F., Demetriou, D. M., and Yocum, C. F. (1987) *Biochim. Biophys. Acta* **891,** 15–21
22. Eidsness, M. K., Burden, A. E., Richie, K. A., Kurtz, D. M., Jr., Scott, R. A., Smith, E. T., Ichiye, T., Beard, B., Min, T., and Kang C. (1999) *Biochemistry* **38,** 14803–14809
23. Miller, A.-F., and Brudvig, G. W. (1991) *Biochim. Biophys. Acta* **1056,** 1–18
24. Meurer, J., Plucken, H., Kowallik, K. V., and Westhoff, P. (1998) *EMBO J.* **17,** 5286–5297
25. Morais, F., Barber, J., and Nixon, P. J. (1998) *J. Biol. Chem.* **273,** 29315–29320
26. Xiao, Z., Maher, M. J., Cross, M., Bond, C. S., Guss, J. M., and Wedd, A. G. (2000) *J. Biol. Inorg. Chem.* **5,** 75–84